JCB Article

Mitochondrial targeting and a novel transmembrane arrest of Alzheimer's amyloid precursor protein impairs mitochondrial function in neuronal cells

Hindupur K. Anandatheerthavarada, Gopa Biswas, Marie-Anne Robin, and Narayan G. Avadhani

Laboratories of Biochemistry, Department of Animal Biology, School of Veterinary Medicine, University of Pennsylvania, Philadelphia, PA 19104

Alzheimer's amyloid precursor protein 695 (APP) is a plasma membrane protein, which is known to be the source of the toxic amyloid β (Aβ) peptide associated with the pathogenesis of Alzheimer's disease (AD). Here we demonstrate that by virtue of its chimeric NH_2-terminal signal, APP is also targeted to mitochondria of cortical neuronal cells and select regions of the brain of a transgenic mouse model for AD. The positively charged residues at 40, 44, and 51 of APP are critical components of the mitochondrial-targeting signal. Chemical cross-linking together with immunoelectron microscopy show that the mitochondrial APP exists in NH_2-terminal inside transmembrane orientation and in contact with mitochondrial translocase proteins. Mutational studies show that the acidic domain, which spans sequence 220–290 of APP, causes the transmembrane arrest with the COOH-terminal 73-kD portion of the protein facing the cytoplasmic side. Accumulation of full-length APP in the mitochondrial compartment in a transmembrane-arrested form, but not lacking the acidic domain, caused mitochondrial dysfunction and impaired energy metabolism. These results show, for the first time, that APP is targeted to neuronal mitochondria under some physiological and pathological conditions.

Introduction

Alzheimer's disease (AD)* is a progressive neurodegenerative disorder involving a number of cellular and biochemical lesions (Mecocci et al., 1996; Sims, 1996; Beal, 1998; Selkoe, 1999). AD is characterized by the deposition of extracellular plaques, which consist of 40–42-amino acid-long amyloid β (Aβ) peptides and intracellular neurofibrilary tangles (Price and Sisodia, 1998; Selkoe, 1999). Aβ peptide is generated from the COOH-terminal end of amyloid precursor protein (APP) by the sequential action of β and γ secretases (Sisodia and St George-Hyslop, 2002). The plasma membrane (PM)–anchored APP in an NH_2 terminus-out and COOH terminus-in orientation (Nunan and Small, 2000) is shown to be the substrate for the β-secretase–mediated processing. The precise cellular site for the γ-secretase–mediated processing remains unclear. The familial or inherited AD, which manifests at an early age, is often associated with mutations in APP, whereas the sporadic form, which manifests at later stages of life, is reported to be multifactorial, including induced expression of APP (Cohen et al., 1988; Palmert et al., 1988; Jacobsen et al., 1991; Rockenstein et al., 1995). Some studies implicate environmental and/or endogenous factors in the pathogenesis of sporadic AD (for review see Hugon et al., 1999). Furthermore, expression of APP is induced by pathological stimuli, environmental factors, and deprivation of tropic factors (Stephenson et al., 1992; Hugon et al., 1999; Shepherd et al., 2000), although intracellular distribution of APP under these conditions remains unknown.

Intracellular lesions, including impairment of mitochondrial energy metabolism, are associated with AD (Sims, 1996; Beal, 1998). A decrease in energy metabolism and altered cytochrome c oxidase (CytOX) activity are among the earliest detectable defects in AD (Parker, 1991; De La Monte et al., 2000; Maurer et al., 2000; Valla et al., 2001). Association

H.K. Anandatheerthavarada and G. Biswas contributed equally to this work.

Address correspondence to Narayan G. Avadhani, Department of Animal Biology, School of Veterinary Medicine, University of Pennsylvania, 3800 Spruce St., #189E, Philadelphia, PA 19104. Tel.: (215) 898-8819. Fax: (215) 573-6651. E-mail: narayan@vet.upenn.edu

*Abbreviations used in this paper: Aβ, amyloid β; AD, Alzheimer's disease; APP, amyloid precursor protein; CytOX, cytochrome c oxidase; DHFR, dihydrofolate reductase; HCN, human cortical neuronal; MTT, methylthiazoletetrazolium; MTX, methatrexate; PM, plasma membrane; TIM, translocase of inner membrane; TOM, translocase of outer membrane.

Key words: amyloid precursor protein; Alzheimer's disease; mitochondrial targeting; transmembrane arrest; mitochondrial dysfunction

of APP with the mitochondrial membrane fraction of AD brains was observed in one study (Yamaguchi et al., 1992), though the precise nature of association or its role in mitochondrial functions were not investigated.

Recently, we showed that xenobiotic inducible cytochromes P4501A1, P4502B1, and P4502E1 proteins contain NH_2-terminal chimeric signals, which enable the bimodal targeting of these predominantly ER proteins to mitochondria as well (Addya et al., 1997; Anandatheerthavarada et al., 1999; Robin et al., 2002). The NH_2-terminal signal sequence of APP resembles the chimeric signals of P4501A1, P4502B1, and P4502E1. We therefore set out to investigate if APP is targeted to mitochondria in addition to the PM. Using human cortical neuronal (HCN-1A) cells, which exhibit in vivo neuronal functions (Ronnett et al., 1990; Dunn et al., 1996), and a transgenic mouse model for AD, we show that human neuronal APP695 is targeted to both the PM and mitochondria. Our results also show that the mitochondrial-targeted APP occurs in a transmembrane-arrested orientation, which affects mitochondrial function and energy metabolism.

Results

Dual localization of APP in human neuronal HCN-1A cells

A comparison of NH_2-terminal chimeric sequences of APP with those of P4501A1 and P4502B1 is shown in Fig. 1 A. The NH_2-terminal 38–amino acid region of APP with a hydrophobic helical structure functions as the ER-targeting domain (Fig. 1 A). Immediately COOH terminal to this region contains positively charged residues at positions 40, 44, and 51 that mimic the cryptic mitochondrial-targeting signals of P4501A1 and P4502B1 (Fig. 1 A). The positively charged residues within sequence 20–30 of P4502B1 and sequence 32–44 of P4501A1 have been shown to be critical for mitochondrial targeting (Addya et al., 1997; Anandatheerthavarada et al., 1999).

The purity of subcellular fractions was established by immunoblot analysis of various membrane fractions from HCN-1A cells using antibodies to Na^+/K^+ ATPase (PM specific), TOM40 (mitochondria specific), calreticulin (ER specific), βCOP (Golgi specific), and p97 (nuclear specific) as markers (Fig. 1 B). Immunoblot analysis using APP Nt Ab (antibody specific for the NH_2-terminal amino acids 42–66) in the bottom panel of Fig. 1 B shows the endogenous levels of 95-kD APP in mitochondria and ~110-kD APP in the PM, ER, as well as Golgi fractions of HCN cells. PMA, a known inducer of APP expression (Ringheim et al., 1996), was used to test the effects of elevated APP on mitochondrial targeting. Northern blot analysis (Fig. 1 C) shows that ~2.1-kb APP695 mRNA was induced at 12 and 24 h of PMA treatment (Fig. 1 C). Although not shown, mRNAs for APP770, APP751, and APLP2 were not detectable by the Northern blot using isoform-specific probes (Shepherd et al., 2000). These results suggest that HCN-1A

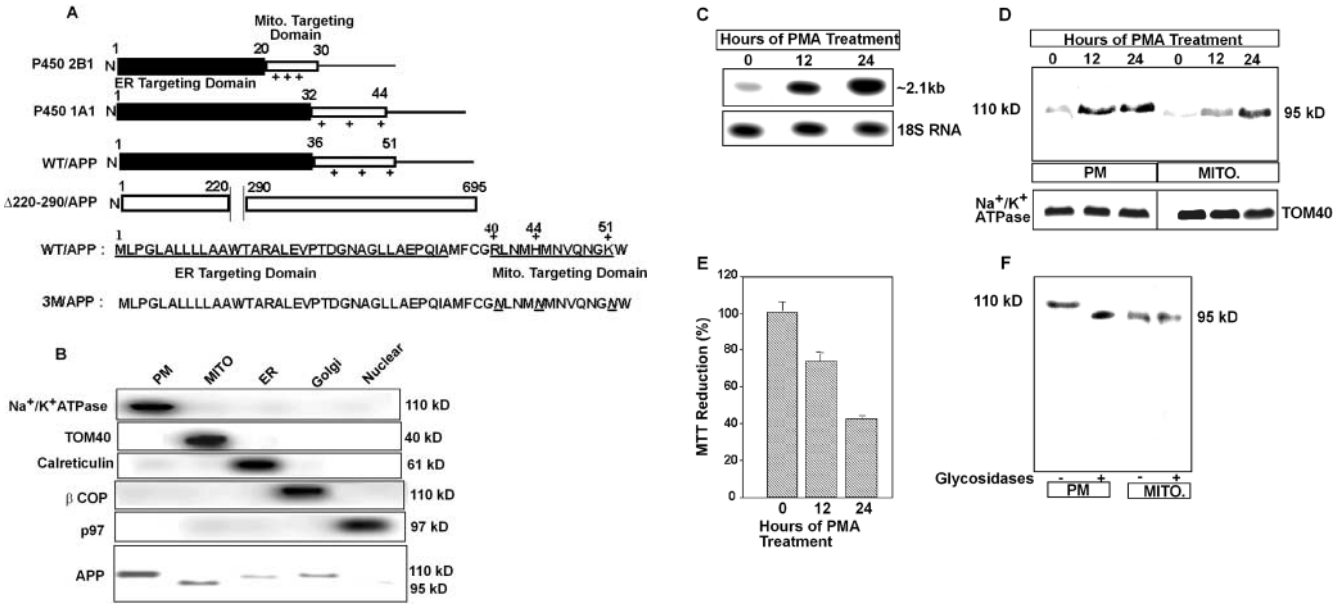

Figure 1. **Chimeric signal properties of APP and its bimodal targeting to mitochondria and PMs.** (A) Chimeric signals of APP and comparison with the signal domains of P4501A1 and 2B1. The ER-targeting sequence (1–36) of APP is indicated as a dark shaded area. Sequence 36–61 with three positively charged residues (at positions 40, 44, and 51), the predicted mitochondrial-targeting sequence, and the mutant construct 3M/APP carrying mutations at these positions are shown. (B) Immunoblot analysis of marker proteins for different subcellular fractions (50 μg protein each) using antibodies to Na^+/K^+ ATPase, TOM40, calreticulin, βCOP, and p97. The bottom panel represents 200 μg protein from each membrane fraction and was developed with APP Nt Ab. (C) Northern blot analysis of total RNA (25 μg RNA each) from HCN cells treated with PMA for different time intervals. Hybridization with 18S DNA probe served as a loading control. (D) Western blot analysis of mitochondria and PM proteins (200 μg protein each) from HCN cells treated with PMA for different time intervals using APP Nt Ab. (E) Measurement of reduction of MTT dye by freshly isolated mitochondria from HCN-1A cells treated with PMA for various time points was performed as described in the Materials and methods. (F) Immunoblot analysis of glycosidase-treated proteins (200 μg each) from PMA (100 nM)-induced HCN cells using APP Nt Ab. Treatment with glycosidases was performed as described in the Materials and methods. Mito, mitochondria.

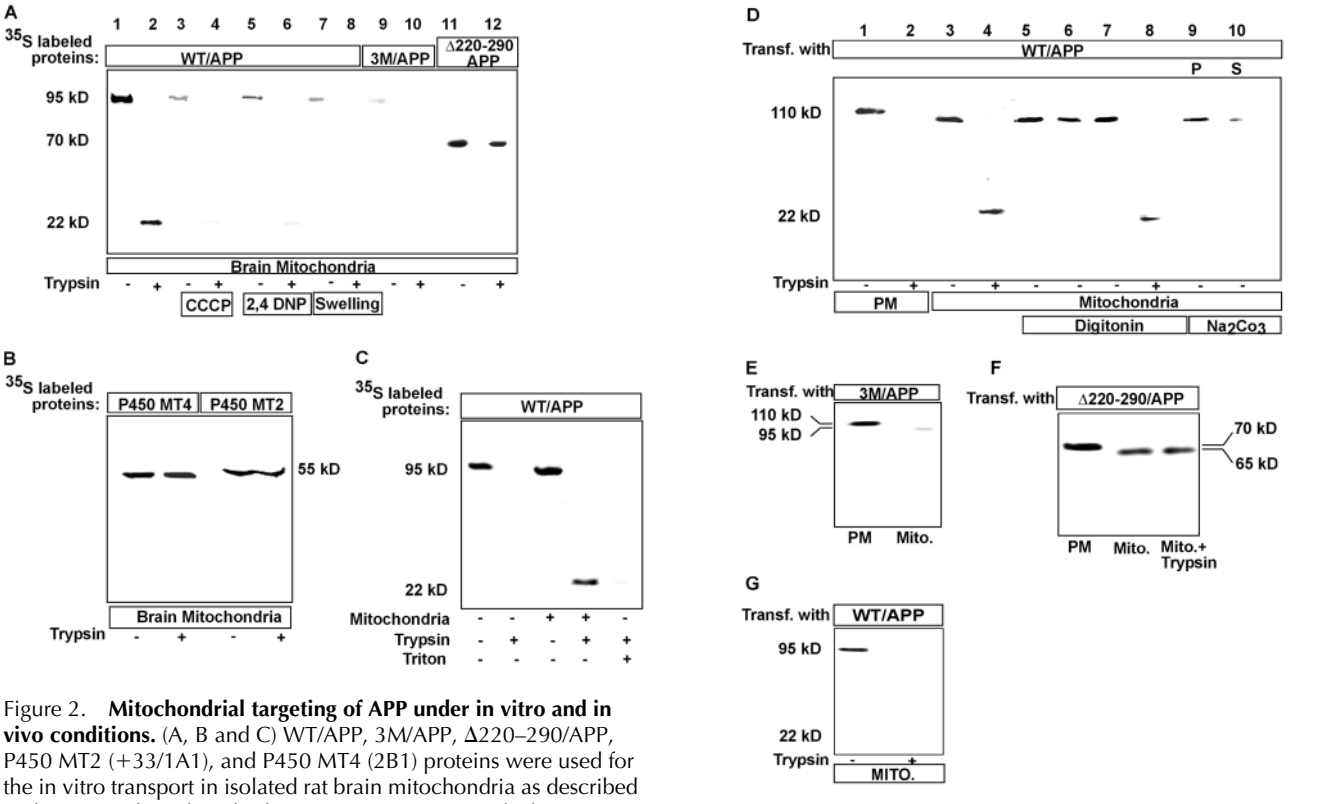

Figure 2. **Mitochondrial targeting of APP under in vitro and in vivo conditions.** (A, B and C) WT/APP, 3M/APP, Δ220–290/APP, P450 MT2 (+33/1A1), and P450 MT4 (2B1) proteins were used for the in vitro transport in isolated rat brain mitochondria as described in the Materials and methods using 250 μg trypsin/ml of reaction (+). (A, lanes 4–6) Mitochondria were preincubated with or without added inhibitors (50 μM CCCP or 50 μM 2,4 DNP) at 25°C for 10 min before initiating the in vitro transport. (C) Mitochondria were treated with 0.1% Triton X-100 before treatment with trypsin. In each case, 200 μg of mitochondrial protein was used for electrophoresis, and the gels were subjected to fluorography. (D–G) In vivo targeting of WT/APP, 3M/APP, and Δ220–290/APP. HCN-1A cells were transfected with WT/APP (D and G), 3M/APP (E), and Δ220–290/APP (F) cDNA constructs, and PM and mitochondrial fractions were probed with APP Ct Ab (D–F) and APP Nt Ab (G). Trypsin treatment was performed as in A. Treatment with digitonin and extraction with 0.1 M Na_2CO_3 (D, lanes 9 and 10) were performed as described in the Materials and methods. P, pellet; S, supernatant.

cells express predominantly the APP695 species. Consistent with induced mRNA levels, the antibody-reactive protein in both PM and mitochondria increased by 10–15-fold by PMA treatment (Fig. 1 D). At 24 h of treatment, the mitochondrial level was nearly 60% of that detected in the PM. Coincident with increased mitochondrial accumulation of APP, the ability of mitochondria to reduce methylthiazole-tetrazolium (MTT), which is widely used as a measure of mitochondrial function, was also progressively diminished (Fig. 1 E).

Immunoblot in Fig. 1 F shows that the 110-kD protein associated with the PM is converted to a 95-kD species after treatment with glycosidases (PNGase F and *O*-glycanase). APP associated with the mitochondrial fraction, on the other hand, did not show any difference in size by these treatments. These results show that a substantial amount (~25–30%) of induced APP695 protein exists in association with the mitochondrial fraction in a nonglycosylated form.

The chimeric NH_2-terminal signal of APP and its incomplete translocation through mitochondrial membranes

The nature of mitochondrial targeting of APP695 was further studied using an in vitro mitochondrial import assay, in which protection against limited proteolytic digestion was used as a criterion for the import of ^{35}S-labeled proteins into mitochondria. Fig. 2 A (lane 1) shows that a full-length APP of 95 kD is recovered in a reisolated mitochondrial fraction after in vitro incubation, suggesting that APP indeed associates with mitochondrial membrane. Trypsin treatment of in vitro–incubated mitochondria resulted in the protection of a 22-kD fragment of APP (Fig. 2 A, lane 2). These results suggest that the 22-kD protected region of APP is located inside the mitochondrial membrane, whereas the remaining ~73-kD portion might be exposed outside. Under similar import conditions, however, the full-length P4501A1 and 2B1 proteins were protected, indicating their complete translocation (Fig. 2 B). Both APP binding to mitochondria and partial internalization were markedly inhibited by uncouplers of mitochondrial membrane potential, CCCP and 2,4 DNP, and also by mitochondrial swelling (Fig. 2 A, lanes 3–8). Furthermore, 3M/APP with mutated positive residues at +40, +44, and +51, as shown in Fig. 1 A, was not imported significantly (Fig. 2 A, lanes 9 and 10), suggesting the importance of these residues for mitochondrial targeting. The possibility of the acidic domain spanning amino acids 220–290 imposing a barrier for complete translocation was verified by using a deletion mutant of APP lacking this domain (Fig. 1 A, Δ220–290/APP). The Δ220–290/APP protein was com-

pletely internalized by mitochondria, as indicated by the protection of nearly the full-length of input protein by trypsin (Fig. 2 A, lanes 11 and 12). Control experiments in Fig. 2 C show that the 22-kD protease-protected fragment is located inside the mitochondrial membranes because disruption of membrane by Triton X-100 (0.1%) rendered the protein sensitive to protease. Furthermore, labeled APP protein in reactions without added mitochondria was completely sensitive to trypsin, dispelling the possibility that resistance to protease was due to some unusual structural features of the protein. These results together show that APP is targeted to mitochondria, although the acidic domain containing 70 negatively charged residues likely imposes a structural barrier for the complete translocation of APP into the mitochondrial compartment.

The bimodal targeting of APP695 in vivo was studied by transfection of HCN-1A neuronal cells with WT/APP, 3M/APP, and Δ220–290/APP cDNAs. PM and mitochondrial proteins from transfected cells were subjected to immunoblot analysis. Both intact and digitonin-treated mitochondria from transfected cells contained significant putative nonglycosylated 95-kD APP (25–30% of the total pool; Fig. 2 D, lanes 3 and 5–7). Mitochondria treated with trypsin showed a 22-kD antibody-reactive fragment (lane 4). Digitonin treatment, which strips off the outer membrane, did not reduce the level of 95-kD protein (Fig. 2 D, lanes 5–7), suggesting its association with the inner membrane matrix compartment. Trypsin treatment of digitonin-treated mitochondria resulted in a slight reduction in the size of protected fragment by ~1–2 kD (Fig. 2 D, lane 8), which may account for the region spanning the intermembrane space of translocation-arrested protein. Resistance to alkaline Na_2CO_3 extraction (Fig. 2 D, lanes 9 and 10) of mitochondrial-associated APP further supports its transmembrane topology. Mutations targeted to the three positively charged residues (3M/APP) completely abolished mitochondrial targeting, though the mutant protein was efficiently targeted to the PM (Fig. 2 E). A deletion construct lacking the acidic domain (Δ220–290/APP), however, was targeted to both the PM and mitochondria (Fig. 2 F). In agreement with the results of in vitro mitochondrial import in Fig. 2 A, the entire length of the Δ220–290/APP protein was protected by protease treatment, suggesting that it is completely internalized by mitochondria (Fig. 2 F, last lane). Finally, the C_{out} orientation of the mitochondrial transmembrane-arrested APP was verified using an antibody specific for the COOH-terminal end of APP (APP Ct Ab). As shown in Fig. 2 G, APP Ct Ab cross-reacted with intact 95-kD mitochondrially associated APP but failed to interact with the protease-protected 22-kD fragment, confirming the N_{in} orientation. These results further demonstrate that mitochondrially targeted APP occurs in a transmembrane-arrested orientation with the NH_2 terminus buried inside mitochondria.

The dual localization of APP695 in mitochondria and the PM was further investigated by immuno-colocalization of

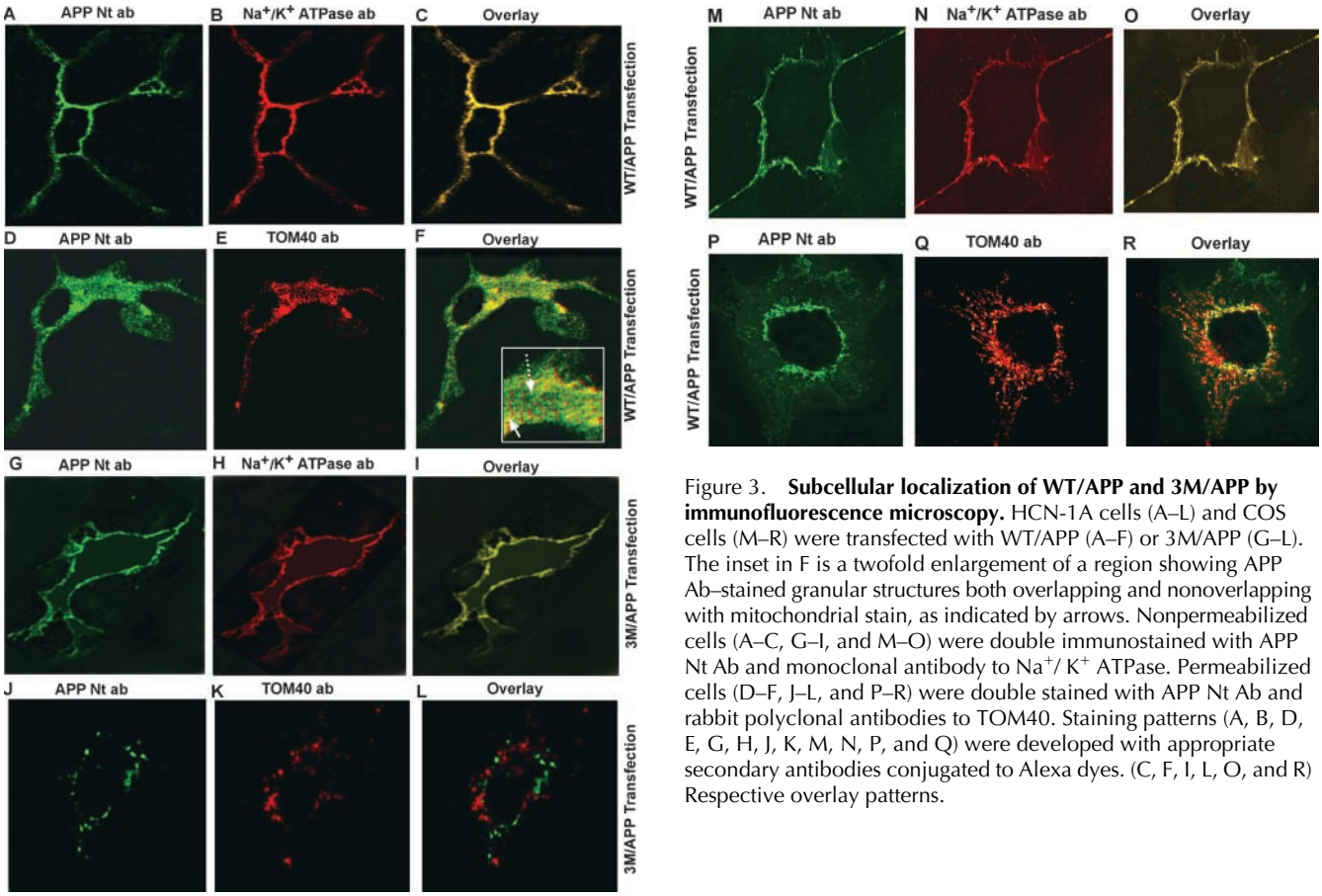

Figure 3. **Subcellular localization of WT/APP and 3M/APP by immunofluorescence microscopy.** HCN-1A cells (A–L) and COS cells (M–R) were transfected with WT/APP (A–F) or 3M/APP (G–L). The inset in F is a twofold enlargement of a region showing APP Ab–stained granular structures both overlapping and nonoverlapping with mitochondrial stain, as indicated by arrows. Nonpermeabilized cells (A–C, G–I, and M–O) were double immunostained with APP Nt Ab and monoclonal antibody to Na^+/K^+ ATPase. Permeabilized cells (D–F, J–L, and P–R) were double stained with APP Nt Ab and rabbit polyclonal antibodies to TOM40. Staining patterns (A, B, D, E, G, H, J, K, M, N, P, and Q) were developed with appropriate secondary antibodies conjugated to Alexa dyes. (C, F, I, L, O, and R) Respective overlay patterns.

the protein in HCN-1A cells transfected with WT/APP and 3M/APP cDNA constructs for 24 h. Triton-permeabilized cells were subjected to double immunostaining with APP Nt Ab and antibody to mitochondrial outer membrane receptor TOM40. Nonpermeabilized cells were immunostained with APP Nt Ab and antibody to the PM-specific marker Na^+/K^+ ATPase. In nonpermeabilized cells transfected with WT/APP, a robust staining around the PM by APP antibody was observed (Fig. 3 A), which colocalized with Na^+/K^+ ATPase (Fig. 3, B and C). In permeabilized cells, the APP Nt Ab stained extranuclear granulate structures (Fig. 3 D), some of which colocalized with mitochondrial-specific marker TOM40 (Fig. 3, E and F). The inset in Fig. 3 F shows a region of the cell with high mitochondrial content, which shows APP-stained structures both overlapping and nonoverlapping with mitochondrial-specific stain. These results show that ectopically expressed APP is targeted to both the PM (through the ER route) and mitochondria. Predictably, transfection with 3M/APP cDNA yielded predominantly PM-specific staining (Fig. 3, G–I) and also some intracellular staining that did not colocalize with TOM40 stains (Fig. 3, J–L). The level of accumulation of APP in the Golgi apparatus after 48 h of transfection was generally higher in HCN-1A cells overexpressing WT/APP than in cells overexpressing 3M/APP (unpublished data). Reasons for this difference currently remain unclear.

The generality of observations with HCN-1A cells were tested in COS cells transfected with WT/APP cDNA for 24 h. As expected, in intact cells, the antibody stained the PM fraction similar to that in HCN-1A cells (Fig. 3, M–O). In permeabilized cells, the APP Nt Ab stained extranuclear punctuate structures, which colocalized with mitochondrial-specific marker TOM40 (Fig. 3, P–R). Although not shown, immunoblot analysis showed the presence of a 95-kD antibody-reactive protein in mitochondria from transfected COS cells. A more punctate mitochondrial staining was observed in COS cells versus more granular structures in HCN-1A cells, probably reflecting cell-specific differences.

Association of transmembrane-arrested APP with mitochondrial translocases

Interaction of nascent proteins with mitochondrial outer and inner membrane translocase complexes (TOMs and TIMs, respectively) is a critical requirement for mitochondrial import of proteins. Because of the dynamic nature of the transport process, the association of nascent proteins with TOMs and TIMs is detectable only by generating translocation intermediates using fusion proteins with dihydrofolate reductase (DHFR) in the presence of added methatrexate (MTX), a ligand of DHFR (Eilers and Schatz, 1986). To test the association of APP with translocase proteins, we generated a fusion construct consisting of the 1–220 amino acid region of APP fused to DHFR (Fig. 4 A). As shown in Fig. 4 A, the 20-kD DHFR is not imported significantly into mitochondria. However, the 1–220/APP–DHFR fusion protein (42 kD) is imported into mitochondria and rendered resistant to trypsin. In a reaction mixture with added MTX, a 22-kD fragment of the fusion protein is protected, suggesting that only part of the fusion protein enters due to the ligand-mediated translocation arrest.

Fig. 4 B shows the extent of interaction of the 1–220/APP–DHFR fusion protein with various translocase proteins, as determined by chemical cross-linking followed by immunoprecipitation. The fusion protein from an in vitro reaction mixture without added cross-linker is immunoprecipitated by APP Nt Ab but not by pre-immune Ab. The APP Nt Ab also yielded a 42-kD immunoprecipitate with no detectable cross-linked product from a reaction mixture without added MTX, probably reflecting the dynamic nature of the import process. A reaction mixture with added MTX, however, yielded two major cross-linked products (82 and 62 kD) in addition to the 42-kD input protein with Nt Ab. The 82- and 62-kD products were not seen in reactions without added cross-linker. Immunoprecipitation with antibodies specific for different translocase proteins shows that the 82-kD band represents cross-linked products with TOM40 and TIM44, both of which have nearly comparable molecular mass. The 62-kD component represents cross-linked product with TIM23. These results show that the NH_2-terminal 220–amino acid sequence of APP can indeed direct the mitochondrial targeting of a nonmitochondrial reporter protein, DHFR, and that it interacts with mitochondrial translocase proteins.

Fig. 4 C shows the cross-linked products of translocation-arrested APP with mitochondrial translocase complexes. It is seen that reaction with Δ220–290/APP, which is transported into mitochondria without any translocation arrest, predominantly yielded the input protein without any detectable higher molecular forms. Reactions with WT/APP, on the other hand, yielded three higher molecular weight components of ~110, 120, and 140 kD with APP Nt Ab. Immunoprecipitation with antibodies against specific translocase proteins indicated that the 140-kD species consists of APP cross-linked to TOM40 or TIM44, whereas the 120-kD species represents cross-linked product with TIM23. The nature of the 110-kD species remains unclear, though it may represent cross-linked products with some of the smaller TOM or TIM proteins. These results provide confirmatory evidence that the mitochondrial-associated WT/APP exists in transmembrane-arrested form in association with various translocase proteins.

A direct evidence for the transmembrane orientation of mitochondrial-targeted APP was sought by immunoelectron microscopy of HCN-1A cells transfected with WT and mutant APP cDNAs for 32 h. We used primary antibodies specific for the NH_2 and COOH termini of APP and antibody for TOM40 simultaneously for probing the sections, and costained with colloidal gold–conjugated secondary antibodies, each specific for a given antibody. The anti–Nt APP Ab was conjugated to 5-nm gold particles, anti–Aβ APP Ab to 10-nm gold, and anti-TOM40 Ab to 20-nm gold particles. The electron micrograph in Fig. 4 D shows that APP-specific (5 and 10 nm) electron-dense particles are associated with mitochondria, the ER, the Golgi apparatus, and secretory vesicles. Interestingly, the mitochondrial-associated APP is organized in an N_{in}–C_{out} orientation invariably in close proximity to TOM40 protein (20-nm particle). The positions of the NH_2- and COOH-terminal–specific stains suggest that the APP protein is in direct contact with, and possibly traversing, the channel-forming

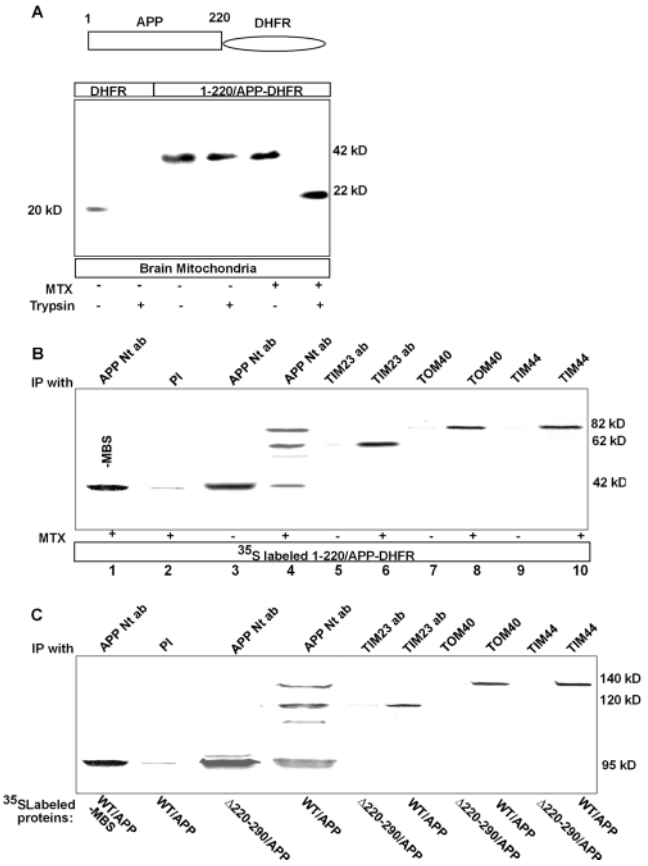

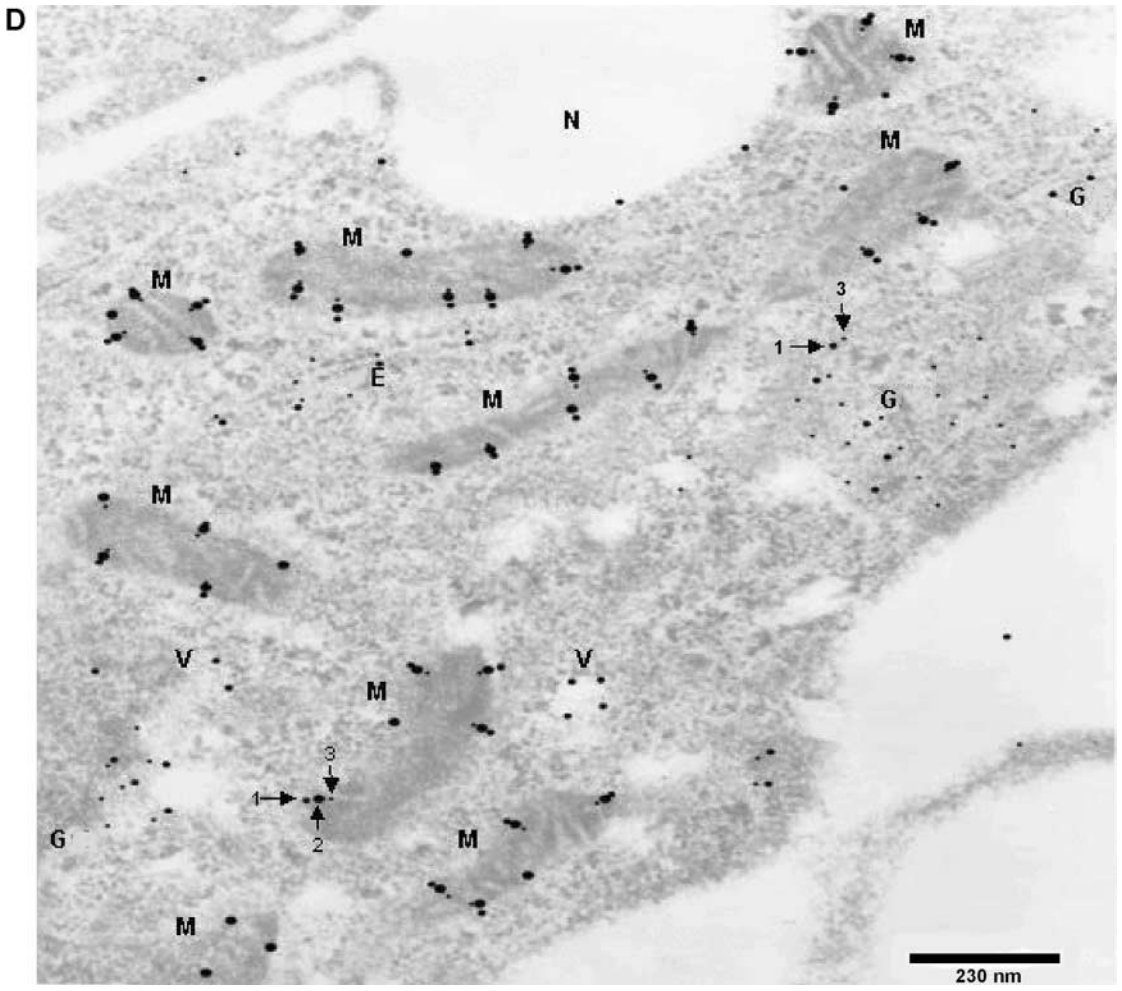

Figure 4. **Transmembrane-arrested APP exists in contact with mitochondrial translocase proteins.** ^{35}S-labeled APP (1–220) fused to DHFR (APP–DHFR), WT/APP, or Δ220–290/APP proteins were used for in vitro transport with isolated yeast mitochondria, and translocation intermediates were cross-linked with MBS as described below. In indicated experiments, MTX (1 μmol/ml of reaction) was added to generate translocation intermediates. Both the input and cross-linked products were immunoprecipitated with antibody to APP and then probed with indicated antibodies by immunoblot analysis. (A) In vitro transport of APP–DHFR fusion protein. Trypsin treatment (250 μg /ml reaction) was performed for 20 min on ice as described in the Materials and methods. (B) Cross-linking of APP–DHFR fusion protein with yeast mitochondrial translocases. (C) Cross-linking of WT/APP and Δ220–290/APP with yeast mitochondrial translocase proteins. In vitro transport was performed with indicated proteins in the absence of added MTX. (D, E, and F) Immunoelectron microscopy of HCN-1A cells transfected with WT/APP, 3MAPP, and Δ22–290/APP, respectively, for 32 h. M, mitochondrion; G, Golgi; E, ER; N, nucleus; V, vesicles. Arrow 1, COOH terminus of APP (10-nm gold particle); arrow 2, TOM40 (20-nm gold particle); arrow 3, NH_2 terminus of APP (5-nm gold particle).

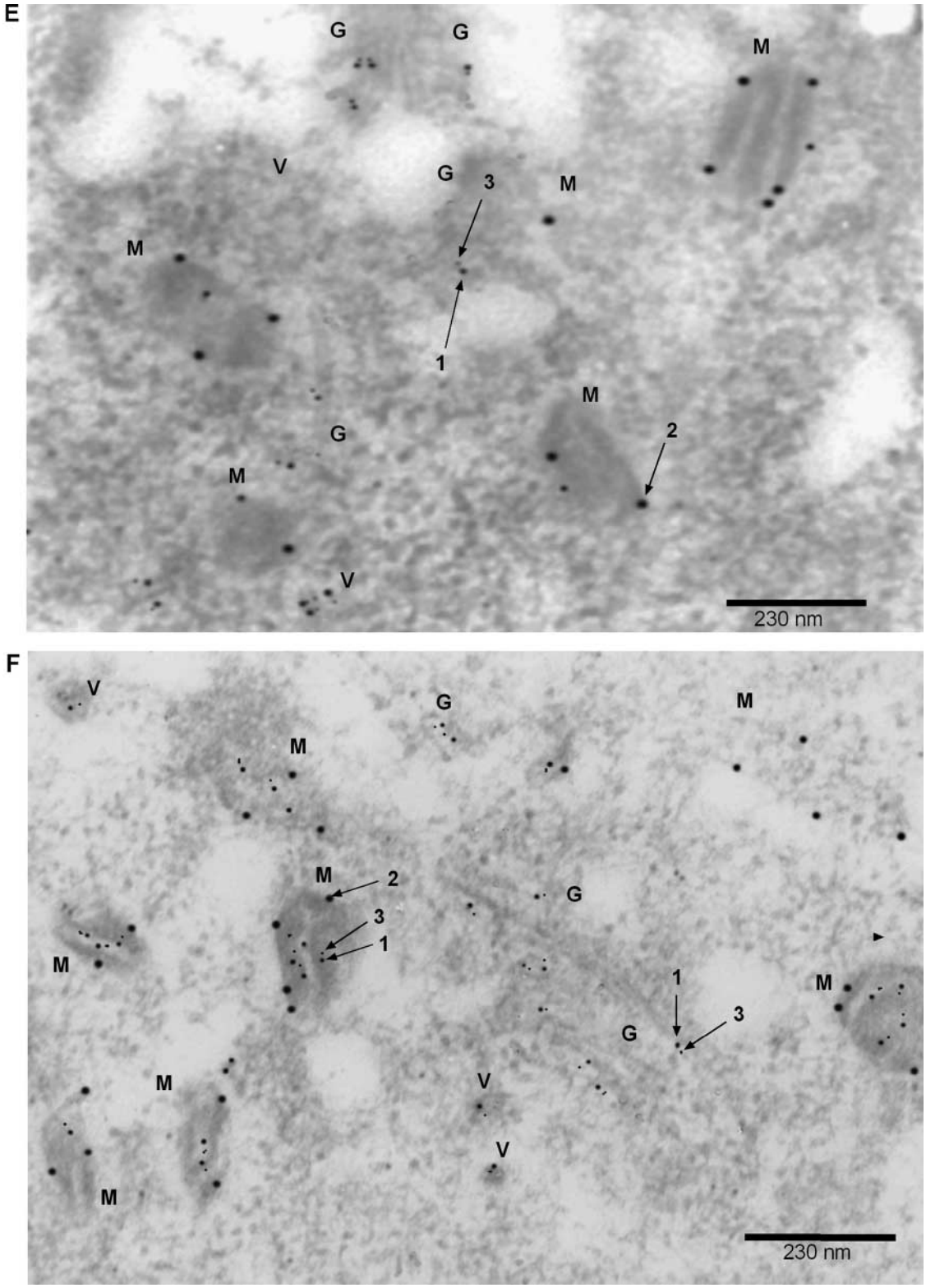

TOM40 protein. As expected, APP associated with the Golgi apparatus, the ER, and secretory vesicles showed only APP NH_2- (Fig. 4 D, arrow 3) and COOH-terminal Aβ (Fig. 4 D, arrow 1)–specific stains, but not TOM40-specific stain. In keeping with the results of immunoblot analysis and immunofluorescence microscopy (Fig. 2 E and Fig. 3, J–L), cells transfected with 3M/APP cDNA showed vastly reduced mitochondrial localization but significant localization in the Golgi apparatus and transport vesicles (Fig. 4 E). Cells transfected with Δ220–290/APP, on the other hand, showed the distribution of COOH- (Fig. 4 E, arrow 1) and NH_2-terminal (Fig. 4 E, arrow 3)–specific stains in different subcellular compartments, including mitochondria (Fig. 4 F). Interestingly, both the COOH- and NH_2-terminal–specific stains for Δ220–290/APP protein were localized well inside the mitochondrial inner membrane,

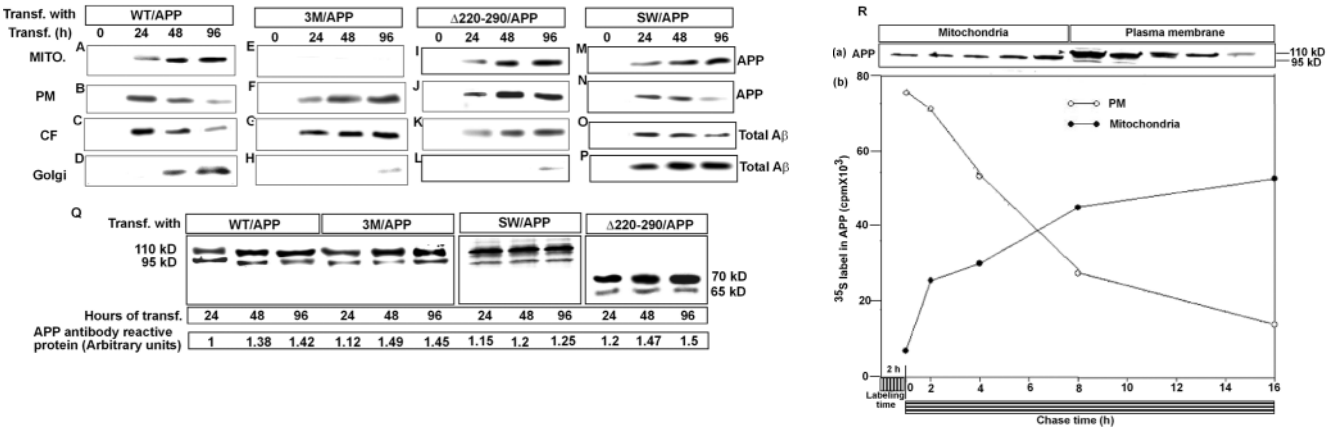

Figure 5. **Subcellular distribution of ectopically expressed APPs in HCN-1A cells.** Cells were transfected with WT/APP (A–D), 3M/APP (E–H), Δ220–290/APP (I–L), and SW/APP (M–P). At indicated times after transfection, mitochondria (MITO.), PM, and Golgi fractions (50 μg protein each) and also protein concentrate from 10 ml of cell-free culture medium (CM) were subjected to Western immunoblot analysis using antibodies to APP Nt (A, B, E, F, I, J, M, and N) or Aβ (C, D, G, H, K, L, O, and P). (Q) The level of expression of total APP protein in cells transfected with various cDNA constructs for different time points was monitored by immunoblot analysis of whole cell lysates. The antibody-reactive proteins were quantified using a Bio-Rad Laboratories Fluoro S imaging system. Table I shows the distribution of APP in different membrane fractions at different time points after transfection with WT/APP and SW/APP cDNAs. Values at the bottom of Q show relative APP levels in comparison with the level at 24-h transfection that was considered to be 1. (R) Pulse chase characteristics of mitochondrial- and PM-associated APP. HCN-1A cells transfected with WT/APP cDNA for 24 h were labeled with [^{35}S]Met for 2 h, followed by a chase in normal growth medium containing 3 mM unlabeled Met. Mitochondrial and PM proteins from cells at different points of chase (500 μg each) were immunoprecipitated with APP Nt Ab, analyzed by electrophoresis on 10% SDS-polyacrylamide gels, and imaged through a Bio-Rad Laboratories GS525 molecular imager. The immunoblot at the top of the figure was performed using 100 μg protein from each fraction using APP Nt Ab.

confirming that it is completely internalized. These results show that mitochondrial-associated APP exists in a translocation-arrested orientation through the mitochondrial membrane. Results also provide further confirmation that the negatively charged domain is essential for causing the translocation arrest of APP.

Inverse patterns of APP accumulation in the mitochondrial and PM fractions at longer time intervals

We next determined the time course of accumulation of APP695 in the mitochondrial and PM fractions of HCN cells transfected with WT/APP, 3M/APP, and Δ220–290/APP cDNA constructs and also the accumulation of the intra- as well as the extracellular Aβ peptide at these time points (Fig. 5; Table I). Immunoblot in Fig. 5 A shows a steady increase in the level of WT/APP in the mitochondrial fraction from 0 to 96 h of transfection, whereas the level in the PM declined steadily during this time (Fig. 5 B). Notably, the level of secreted Aβ pool (Aβ40, 42, and 43) in the culture fluid (CF) declined steadily (Fig. 5 C), in parallel to declining APP in the PM fraction (Fig. 5 B). Use of peptide-specific antibodies to Aβ40 and Aβ42 indicated that cells transfected with 3M/APP cDNA excreted mostly Aβ40 peptide, whereas cells transfected with WT/APP cDNA excreted a mixture of Aβ40 and 42 peptides after 24 h (unpublished data). In cells transfected with 3M/APP, however, no significant mitochondrial accumulation of APP was observed (Fig. 5 E), though the level of PM-associated APP and the secreted Aβ peptide (Fig. 5, F and G) increased with time. Furthermore, cells transfected with Δ220–290/APP showed a time-dependent increase in the accumulation of mutant protein in both the mitochondrial (Fig. 5 I) and PM (Fig. 5 J) compartments. This coincided with the increased secretion of total Aβ in the culture fluid (CF) (Fig. 5 K). As the Golgi network has been shown to be an important cellular site of Aβ production (Greenfield et al., 1999), we examined the level of the Aβ peptide in the purified Golgi fraction of transfected cells. It is seen that by 48 h of transfection, there was an increased accumulation of the peptide in the Golgi apparatus of cells transfected with WT/APP (Fig. 5 D). Surprisingly, accumulation of processed 4-kD Aβ peptide in the Golgi apparatus did not occur in cells transfected with 3M/APP and Δ220–290/APP constructs

Table I. **Subcellular distribution of APP in cells transfected with WT/APP and SW/APP constructs**

% Distribution of WT/APP					% Distribution of SW/APP				
Transfection (h)	Mito	PM	CF	Golgi	Transfection (h)	Mito	PM	CF	Golgi
24	14.5	42	43	0.5	24	15	25	35	25
48	32.3	23.3	28	16.4	48	28	15	20	37
96	43	7.7	10	39.3	96	38	3	8	51

The distribution of antibody-reactive protein was determined by quantitation of immunoblots from Fig. 5 (A–D and M–P). The sum of band densities (Mito, PM, CF, and Golgi) was taken as 100% for calculating the % distribution. Mito, mitochondria; CF, culture fluid.

(Fig. 5, H and L). We also tested the intracellular distribution of the Swedish mutant of APP (SW/APP), which is implicated in familial AD (Selkoe, 1999). Fig. 5 (M–P) shows that the pattern of accumulation of APP in mitochondria and the PM and the level of secreted Aβ in the extracellular compartment are nearly similar to those with WT/APP. The only difference is the time frame of accumulation of 4-kD Aβ peptide in the Golgi apparatus, which occurs at 24 h in the case of SW/APP and 48 h in the case of WT/APP. These results show that the levels of mitochondrial targeting of WT/APP and SW/APP are nearly similar.

Total cell extracts from companion cells, as in Fig. 5 (A, E, I, and M), were subjected to immunoblot analysis to determine the level of expression of WT and mutant forms of APP at various time points of transfection. Results in Fig. 5 Q show that the levels of expression of WT, 3M/APP, and Δ220–290/APP at all time points were nearly comparable with an ~10–20% increase by 48 and 96 h as compared with the 24 h time point. These results suggest that the observed differences in the distribution of APP and Aβ peptide levels in different cell compartments were not due to vastly variable levels of transfection or expression.

The reason for the contrasting levels of APP in the mitochondrial and PM fractions at longer time intervals was verified by pulse chase experiments. After 24 h of transfection with WT/APP cDNA, cells were labeled for 2 h with [^{35}S]Met and chased for various time periods up to 16 h (Fig. 5 R) by growing in a normal medium. APP protein from the mitochondrial and PM fractions at each time point was immunoprecipitated and resolved on an SDS gel, and the radioactivity was quantified. Fig. 5 R shows that the radioactivity in the mitochondrial-associated APP increased steadily up to 16 h of chase, whereas the radioactivity in the PM fraction declined steadily. The steady-state APP levels in the mitochondrial and PM fractions, as indicated in the immunoblot at the top, essentially concur with the pulse chase pattern. These results show that the pools of APP from the mitochondria and PM are turned over quite differently and provide a rational basis for the observed differences in the steady-state levels of APP in the two compartments at 48 and 96 h after transfection.

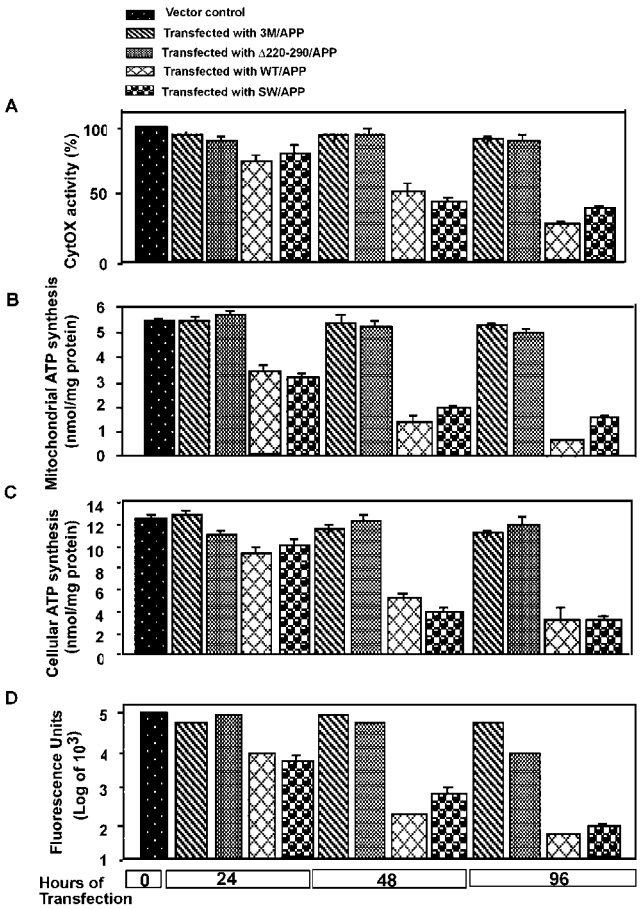

Figure 6. **Effects of transmembrane-arrested APP on mitochondrial functions.** Total cell extracts or mitochondria from HCN-1A cells transfected with WT/APP, 3M/APP, Δ220–290/APP, and SW/APP were analyzed for CytOX activity (A), mitochondria and total cell ATP generation (B and C, respectively), and changes in the mitochondrial membrane potential using MitoTracker orange CM-H_2TM ROS (D), as described in the Materials and methods. Mitochondrial CytOX activity (2 nmol of cytochrome c oxidized/min/mg mitochondrial protein) from vector alone–transfected cells was used as 100% activity. Values represent mean ± SEM from three separate transfection experiments.

Accumulation of transmembrane-arrested APP disrupts mitochondrial functions

To understand the patho-physiological relevance of the mitochondrial accumulation of APP in a transmembrane-arrested orientation, we assessed mitochondrial functional parameters. A time-dependent accumulation of APP in the mitochondria of cells transfected with WT/APP was accompanied by a decline in the CytOX activity (Fig. 6 A), markedly reduced respiration-coupled (mitochondrially generated) ATP synthesis (Fig. 6 B), a decline in total cellular ATP levels (Fig. 6 C), and disruption of mitochondrial transmembrane potential (Fig. 6 D). These functional parameters were progressively reduced to 50–80% of control cells transfected with vector DNA alone (Fig. 6, A–D). Transfection with 3M/APP (which showed no detectable mitochondrial accumulation) and Δ220–290/APP (which did not cause translocational arrest), however, showed no effect on the cellular or mitochondrial ATP pools, CytOX activity, or transmembrane potential (Figs. 6, A–D). Transfection with SW/APP with intact NH_2-terminal signal sequence and the acidic domain affected mitochondrial functional parameters at levels similar to that with WT/APP. These results show, for the first time, the progressive nature of mitochondrial accumulation of transmembrane-arrested APP and its adverse effects on energy production in cells overexpressing the protein.

Transmembrane-arrested APP and impaired energy metabolism in brain mitochondria from a mouse model for AD

AD-like plaque pathology was uniformly observed in transgenic mouse models expressing higher levels of human APP protein (for review see Janus and Westaway, 2001). To understand the physiological significance of our results with transfected cells, we analyzed the subcellular distribution of

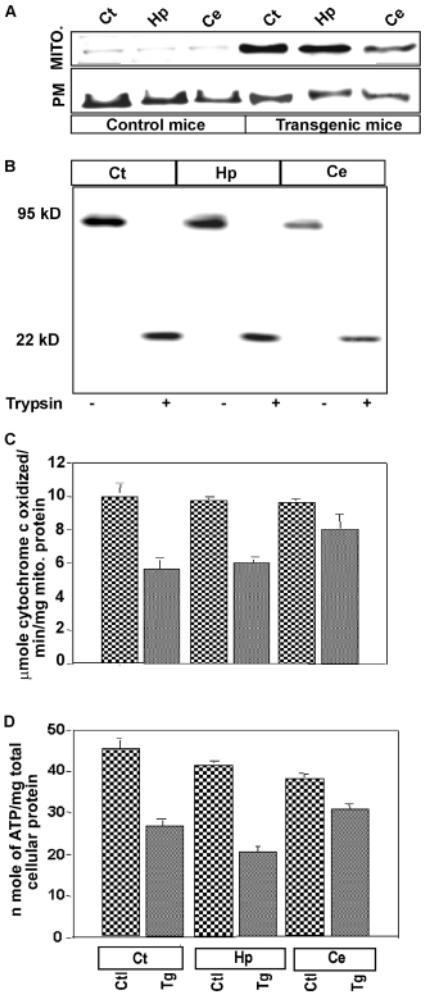

Figure 7. **Mitochondrial-associated APP in the brains of transgenic mice overexpressing APP.** (A) Mitochondria and PM fractions from different brain regions of control and SWEAPP (2576) transgenic mice (50 µg protein each) were subjected to immunoblot analysis using APP Nt Ab. (B) Mitochondria (50 µg) from different brain regions of transgenic mice overexpressing SW/APP (SWEAPP [2576]) were subjected to trypsin treatment (as described in Fig. 2) followed by immunoblot analysis with APP Nt Ab. (C) CytOX activity in total mitochondrial membrane fraction and (D) total cellular ATP levels were assayed as described in the Materials and methods. MITO., mitochondria; Ctl, control; Tg, transgenic; Ct, cortex; Hp, hippocampus; Ce, cerebellum.

APP in the brains of transgenic mice overexpressing SW/APP (2576). PM and mitochondria from cortex, hippocampus, and cerebellum regions of brains from 12-mo-old amyloid plaque–bearing transgenic mice were isolated and compared with similar regions of age-matched controls. The immunoblot in Fig. 7 A (bottom) shows that the antibody-reactive APP levels in the PM from the cortex, hippocampus, and cerebellar regions of brains from control and transgenic mice were nearly comparable. But the mitochondrial fractions of corresponding mouse brain regions of transgenic mice showed markedly elevated APP compared with counterparts from control brains (Fig. 7 A, top). The cortex and hippocampal regions of transgenic mice contained considerably higher levels of mitochondrial-associated APP compared with the cerebellum. Furthermore, trypsin treatment of mitochondria from different brain regions of transgenic mice yielded a 22-kD protected fragment of APP (Fig. 7 B). These results suggest a transmembrane-arrested topology of mitochondrial-associated APP in transgenic mouse brain similar to that observed in HCN-1A cells transfected with WT/APP cDNA. Increased mitochondrial association of APP in the transgenic mouse model was accompanied by a 20–40% decrease in the CytOX activity (Fig. 7 C) and a 25–50% reduction in total cellular ATP levels (Fig. 7 D) in the cortex and hippocampus. The cerebellar region with a relatively lower level of mitochondrial-associated APP showed a less severe inhibition of CytOX activity (Fig. 7 C) and ATP pool (Fig. 7 D). These results confirm that in both APP-expressing HCN-1A cells and mouse brain, mitochondria are the direct targets of this pathogenic protein.

Discussion

AD is associated with multiple lesions including reduced ATP synthesis and altered mitochondrial structure and function in the brain. It is not clear whether the AD-associated mitochondrial defects are contributing factors in the progression of the disease. A general change in glucose utilization, increased oxidative stress, and Ca^{2+} deregulation are additional metabolic defects in the AD brain that may also be associated with defective mitochondrial function (Sims, 1996; Beal, 1998). However, the precise mechanism of mitochondrial pathology in AD remains unclear. In this study, we demonstrate for the first time that incomplete translocation and progressive accumulation of APP on mitochondrial membranes is the major cause of mitochondrial dysfunction.

The APP cDNA constructs and proteins used in this study contained an intact COOH-terminal end, which contributes to the toxic Aβ peptide as mutations were exclusively targeted to the NH_2-terminal signal sequence or the 70–amino acid-long acidic region. Additionally, as shown in Fig. 5 Q, transfection conditions were standardized to yield nearly comparable levels of expression. We also used a nontransformed human neuronal HCN-1A cell line whose neurochemical and morphological characteristics have been well documented. These cells resemble the human primary cortical neuronal cells and are suitable for studying neurodegenerative disorders (Ronnett et al., 1990; Dunn et al., 1996). Essentially similar mitochondrial accumulation of transmembrane-arrested APP and altered mitochondrial oxidative functions were observed in brain regions of a transgenic mouse model for AD, suggesting the physiological relevance of our findings.

The concept of chimeric NH_2-terminal signals that direct the bimodal targeting of proteins to both the ER and mitochondria emerged from our recent studies on the targeting of cytochromes P4501A1, 2B1, and 2E1 (Addya et al., 1997; Anandatheerthavarada et al., 1999; Robin et al., 2002). The prevailing view up to this point was that cytoplasmically translated proteins are targeted either to the ER or to mitochondria by virtue of specific NH_2-terminal signals they carry. In our search for other cellular proteins containing similar bimodal targeting signals, we found that the NH_2 terminus of APP resembles the chimeric signal of

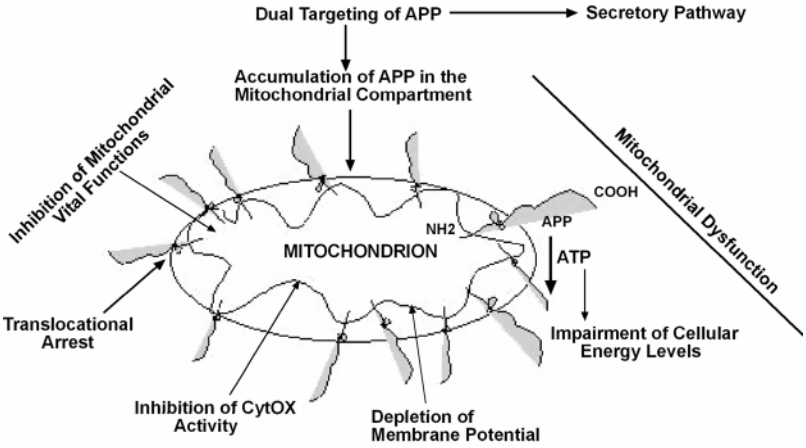

Figure 8. **A proposed model for the mitochondrial targeting and accumulation of transmembrane-arrested APP affecting mitochondrial functions.**

P4501A1, 2B1, and 2E1. Our results using both in vivo targeting by ectopic expression of APP in whole cells as well as in vitro transport in isolated brain mitochondria demonstrate that the three positively charged residues at +40, +44, and +51 of APP are critical for mitochondrial targeting. Mitochondrial localization of APP in transiently transfected HCN-1A cells is not an artifact of overexpression, as PMA-mediated induction of endogenous gene expression in HCN-1A cells resulted in the accumulation of APP in the mitochondrial compartment and a corresponding inhibition of mitochondrial function. Translocation-arrested APP–DHFR fusion protein interacts efficiently with mitochondrial inner and outer membrane translocase proteins TOM40, TIM23, and TIM44 (Truscott et al., 2001), as tested by chemical cross-linking, which provides direct support for mitochondrial targeting of APP. A similar mitochondrial transmembrane-arrested APP pool and altered mitochondrial function were observed in brains of APP-overexpressing mice that have been used as models for AD. Furthermore, mitochondrial targeting of APP is not restricted to neuronal cells because COS cells overexpressing this protein also show mitochondrial localization.

Protection of a 22-kD fragment against proteolytic digestion initially suggested that the mitochondrially targeted APP in HCN-1A cells as well as in the brains of transgenic mice exists in a translocation-arrested orientation. The arrest region maps to the 70–amino acid-long acidic domain, which is implicated in Zn^{2+} binding and functional interaction with other proteins (Takahashi et al., 2000). The trans-mitochondrial membrane arrest and also the role of the acidic domain in causing the arrest were investigated by two different approaches. In the first approach, the use of WT/APP with an intact acidic domain for in vitro import into isolated mitochondria yielded translocation intermediates that could be cross-linked with mitochondrial inner and outer membrane translocases (Fig. 5 C). The Δ220–290/APP protein with deleted acidic domain, on the other hand, failed to produce cross-linked products with translocase proteins, suggesting the role of the acidic domain in translocation arrest. The second approach involved immunoelectron microscopy of transfected HCN-1A cells, which demonstrates contrasting modes of mitochondrial membrane association of WT/APP and Δ220–290/APP, lacking the acidic domain. Results conclusively show that mitochondrial-targeted APP exists in an N_{in}–C_{out} transmembrane-arrested topology and that transmembrane-arrested protein is either in direct contact with, or traversing through, TOM40 translocase. The immunoelectron microscopy results (Fig. 4 D) show that nearly 80% of antibody-stained TOM40 complexes along the mitochondrial outer membrane are engaged by APP. These results lead us to believe that blocking of mitochondrial protein transport channels by transmembrane-arrested APP is a major contributing factor in the impairment of mitochondrial functions and decreased cellular energy levels. In support of this view, NH_2-terminal mutations that affected mitochondrial targeting or deletion of the acidic domain that abolishes translocation arrest did not cause adverse effects on any of the mitochondrial functions tested. This is probably the first demonstration of translocation arrest causing mitochondrial perturbation in any biological system. We believe that the structural features of this domain impose a barrier for complete translocation. The inability of cytoplasmic chaperones to fully unfold the polypeptide at this domain might be the cause of translocation arrest of APP. An alternative possibility is that the negatively charged domain fails to bind efficiently to the negatively charged channel-forming outer membrane protein TOM22 because of electrostatic repulsion.

In support of previous studies (Hatanpaa et al., 1998; Webster et al., 1998), our results show that increased production of extracellular Aβ peptide in cells overexpressing the 3M/APP and Δ220–290/APP mutant proteins did not cause changes in mitochondrial function or ATP synthesis. The accumulation of Aβ in the Golgi network might be directly related to reduced APP trafficking to the PM and decreased Aβ secretion in cells transfected with WT/APP. These results are in agreement with the view that accumulation of COOH-terminal fragments in the intracellular compartments impairs Aβ secretion and APP trafficking (Greenfield et al., 1999; Maltese et al., 2001). However, expression of 3M/APP and Δ220–290/APP mutant proteins that failed to cause mitochondrial dysfunction showed no accumulation of Aβ peptides in the Golgi network, suggesting that mitochondrial function may somehow be associated with the accumulation of toxic Aβ peptides in the secretory pathway. Although the precise relationship between mitochondrial injury and altered trafficking of cargo through the Golgi network remains un-

known, our results are in line with a previous study implicating the role of mitochondrial function in the accumulation of COOH-terminal fragments of APP in the secretory pathway (Busciglio et al., 2002). Based on these, we propose a model (Fig. 8) for the bimodal targeting of APP through its NH_2-terminal chimeric signal. We further propose that under increased APP expression, a progressive accumulation of transmembrane-arrested APP causes perturbation of mitochondrial function, which in turn results in impairment of energy metabolism.

Studies on overexpression of WT/APP either by transient transfection or by stable expression in cell types including neuronal cells have noted growth defects and mitochondrial structural abnormalities (Nishimura et al., 1998; Grant et al., 1999; Uetsuki et al., 1999; Campard et al., 2000). It is thought that the threshold of expression of WT/APP needed to cause cellular abnormality is relatively higher than that with APP bearing familial Alzheimer's mutations (Hasimoto et al., 2000). The threshold level of APP expression needed for the pathogenic outcome also appears to be related to species variations, as humans with trisomy express only twofold higher levels of WT/APP and yet invariably develop AD pathology by 30–40 yr of age (Teller et al., 1996). However, a fivefold higher expression of familial AD mutant APP, including SW/APP, is required to induce AD-like pathology in mice (for review see Janus and Westaway, 2001). Results of cDNA transfection in HCN-1A cells (Figs. 5 and 6) show that the extent of mitochondrial targeting and causation of mitochondrial injury are comparable with both WT/APP and SW/APP. It is therefore likely that increased mitochondrial accumulation and associated mitochondrial toxicity are contributing factors in the pathogenesis of the AD-like syndrome in the SW/APP-overexpressing animal model analyzed in this study. In summary, we show a novel mode of APP targeting to mitochondria, which may contribute to the pathogenic outcome, especially in the APP-overexpressing neuronal cells.

Materials and methods

Protein transport into isolated mitochondria

In vitro import of ^{35}S-labeled proteins into isolated rat liver mitochondria was performed as described before (Addya et al., 1997). cDNAs encoding the SW/APP (K595N and M596L), 3M/APP, and Δ220–290/APP were generated using pCB695 as the template and cloned into TA vector. ^{35}S-labeled translation products were generated in a transcription-coupled translation system (Promega). Import of the in vitro–synthesized proteins was performed in a 200-μl volume (Addya et al., 1997), in some cases with added inhibitors CCCP (50 μM) and 2,4 DNP (50 μM). Swelling was caused by suspending mitochondria in a hypotonic buffer (Addya et al., 1997). In vitro–incubated mitochondria were subjected to trypsin treatment (250 μg/ml of reaction) and pelleted through 1 M sucrose. Mitochondrial proteins were separated by SDS-PAGE and subjected to fluorography.

Cell transfection and subcellular localization of proteins

HCN-1A neuronal cells derived from human cortex (American Type Culture Collection) were grown in DME (pH 7.35) containing 4 mM L-glutamate, 1.5 g/L sodium carbonate, and 10% FBS. Cells were transfected with WT/APP, and mutant cDNAs were cloned into mammalian expression vector pCMV4 (5 μg/plate) using Fugene at 50% confluence. Cells were harvested and homogenized (35–40 strokes) in four volumes of homogenization buffer (250 mM sucrose, 10 mM Tris-HCl, pH 7.4, and 1 mM $MgCl_2$) using a Teflon-fitted glass homogenizer. The homogenate was centrifuged at 1,500 *g* for 20 min, and the resulting pellet was used for isolating the PM as previously described (Dasso, 1998). The 1,500 *g* supernatant fraction was used to isolate mitochondria by sucrose density banding as described before (Addya et al., 1997). Golgi and ER fractions were isolated from post-mitochondrial supernatant (Dasso, 1998). The purity of the PM and mitochondrial fraction was assessed by enrichment of marker proteins. In some experiments, mitochondria from transfected cells were subjected to protease protection assay, digitonin fractionation, and 0.1 M Na_2CO_3 (pH 11) extraction as described before (Anandatheerthavarada et al., 1999).

Immunoblot and Northern blot analysis

Proteins were resolved by electrophoresis through 10% SDS-polyacrylamide gels or 12% Tricine gels and transferred to nitrocellulose membrane. Immunoblots were developed with rabbit polyclonal antibodies directed against the COOH-terminal 22–amino acid sequence of APP (APP Ct Ab), the Aβ Ab (Zymed Laboratories) raised against the 1–40/42 Aβ region of APP, or goat polyclonal antibody against sequence 44–63 of APP (APP Nt Ab) (Calbiochem). The blots were developed using the Pierce Super Signal ULTRA chemiluminescence substrate kit, and the protein bands were quantitated in a Bio-Rad Laboratories FluorS imaging system. Total RNA (25 μg) was subjected to Northern hybridization using oligonucleotide probes specific to APP695 (Shepherd et al., 2000) by standard conditions.

Indirect immunofluorescence microscopy

HCN-1A cells grown on coverslips were transfected with various cDNA constructs for 32 h and processed for antibody staining as previously described (Addya et al., 1997). Cells permeabilized with 0.1% Triton X-100 were stained with APP Nt Ab and rabbit polyclonal antibody to TOM40. Nonpermeabilized cells were stained with APP Nt Ab and a mouse monoclonal antibody to Na^+/K^+ ATPase as a marker for PM. The cells were then stained with appropriate fluorescence-tagged secondary antibodies and subjected to confocal fluorescence microscopy (Leica).

Measurement of CytOX activity and ATP levels

ATP levels were measured using a somatic cell ATP assay kit (Sigma-Aldrich). Mitochondria and total cell lysates were mixed with ATP-releasing reagent and assayed for luciferase activity as per the manufacturer's protocol in a TD-20/20 luminometer (Turner Designs). COX activity was measured essentially as previously described using ferrocytochrome c as substrate (Vijayasarathy et al., 1999).

Protein deglycosylation assay

Membrane proteins (200 μg) were deglycosylated in 50 μl of 100 mM Tris-HCl buffer, pH 8.6, with 2 mU of PNGase F (Roche) at 37°C for 12 h. The membranes were reisolated and suspended in 100 mM sodium citrate buffer, pH 6.0, containing 0.1% SDS and 1% NP-40 and 2 mU *O*-glycanase (Roche). After overnight incubation at 37°C, the reaction mixture was mixed with 0.2 volumes of 5× Laemmli's buffer and subjected to SDS-PAGE.

Isolation of brain regions from APP-overexpressing mice

Cortex, hippocampus, and cerebellum were dissected using anatomical landmarks from 12-mo-old transgenic APPSWE (2576) and age-matched control mice (B6SJLF1) purchased from Taconic. Tissue was pooled from three animals from each group. Mitochondria and PM from the pooled tissue were isolated as described above.

MTT reduction assay

The conversion of MTT to formazan by mitochondria was performed according to Duan et al. (1999). Mitochondria (200 μg protein) were incubated with MTT dye (0.5 mg/ml) in a 400-μl reaction volume at 37°C for 90 min. After the incubation, mitochondria were isolated and suspended in DMSO (100%), and the absorbance of the solution was measured spectrophotometrically at 592 nm.

Measurement of mitochondrial membrane potential

Measurements were performed spectrofluorometrically in cell suspension essentially as described by Amuthan et al. (2002). The membrane potential was measured as a function of mitochondrial uptake of MitoTracker orange CM-H_2TM ROS (50 nM) added to the cell suspension. Fluorescence was monitored in a multiwavelength excitation dual wavelength emission Delta RAM PTI spectrofluorometer at 525 nm excitation and 575 nm emission.

Immunoelectron microscopy

HCN-1A cells transfected with various cDNAs for 32 h were fixed in 20 mM phosphate buffer containing 4% formaldehyde and 2% glutaralde-

hyde. Cells were dehydrated through a graded ethanol series and embedded in hard grade LR White resin. Ultrathin sections, mounted on nickel grids, were blocked with 20% FBS in TBS for 30 min at room temperature. The sections were incubated with APP Nt Ab (anti–goat) and APP Aβ Ab (anti–mouse) as well as antibody to TOM40 (anti–rabbit) for 24 h at 4°C. The grids were rinsed with TBST for 15 min and incubated with anti–goat (5 nm), anti–mouse (10 nm), and anti–rabbit (20 nm) colloidal gold–conjugated IgGs. Finally, the grids were stained with a saturated suspension of aqueous uranyl acetate. The sections were examined and photographed in a JEOL JEM-1010 electron microscope.

Metabolic labeling

HCN-1A cells transfected with wild-type APP695 for 24 h were initially labeled with [^{35}S]methionine (400 μCi/ml in methionine-free DME plus 5% dialyzed FBS) for 2 h. This was followed by a change of medium to normal DME with FBS and additional growth for 2–16 h at 37°C. Mitochondria and PM were isolated from cells at each time point of chase, and 500 μg of each protein was immunoprecipitated with antibodies to APP Nt Ab at 4°C by adsorption to protein A–agarose beads (Anandatheerthavarada et al., 1999) and resolved by electrophoresis on 10% SDS-polyacrylamide gels. The gels were dried and imaged through a Bio-Rad Laboratories GS-525 radiometric imager.

We thank Dr. S.S. Sisodia (University of Chicago, Chicago, IL) for providing pCB695 cDNA construct, Ms. Molly Higgins for editorial assistance, Dr. Naresh Babu V. Sepuri (Thomas Jefferson University, Philadelphia, PA) for TIM23 antibodies, Dr. Dorothy G. Flood for helpful discussions, and Ms. Nilima Shaha and the Biomedical Imaging Core Laboratory at the University of Pennsylvania for carrying out the immunoelectron microscopy.

This work was supported by National Institutes of Health grant GM34483.

Submitted: 8 July 2002
Revised: 16 January 2003
Accepted: 10 February 2003

References

Addya, S., H.K. Anandatheerthavarada, G. Biswas, S.V. Bhagwat, J. Mullick, and N.G. Avadhani. 1997. Targeting of NH_2-terminal–processed microsomal protein to mitochondria: a novel pathway for the biogenesis of hepatic mitochondrial P450MT2. *J. Cell Biol.* 139:589–599.

Amuthan, G., G. Biswas, H.K. Anandatheerthavarada, C. Vijayasarathy, H.M. Shephard, and N.G. Avadhani. 2002. Mitochondrial stress-induced calcium signaling, phenotypic changes and invasive behavior in human lung carcinoma A549 cells. *Oncogene.* 21:7839–7849.

Anandatheerthavarada, H.K., G. Biswas, J. Mullick, N.B. Sepuri, L. Otvos, D. Pain, and N.G. Avadhani. 1999. Dual targeting of cytochrome P4502B1 to endoplasmic reticulum and mitochondria involves a novel signal activation by cyclic AMP-dependent phosphorylation at ser128. *EMBO J.* 18:5494–5504.

Beal, M.F. 1998. Mitochondrial dysfunction in neurodegenerative diseases. *Biochim. Biophys. Acta.* 1366:211–223.

Busciglio, J., A. Pelsman, C. Wong, G. Pigino, M. Yuan, H. Mori, and B.A. Yankner. 2002. Altered metabolism of the amyloid β precursor protein is associated with mitochondrial dysfunction in Down's syndrome. *Neuron.* 33:677–688.

Campard, P.K., B. Tasiaux, and J.N. Octave. 2000. The processing and biological function of the human amyloid precursor protein (APP): lessons from different cellular models. *Exp. Gerontol.* 35:843–850.

Cohen, M.L., T.E. Golde, M.F. Usiak, L.H. Younkin, and S.G. Younkin. 1988. In situ hybridization of nucleus basalis neurons shows increased β-amyloid mRNA in Alzheimer's disease. *Proc. Natl. Acad. Sci. USA.* 85:1227–1231.

Dasso, M. 1998. In vitro reconstitution. *In* Current Protocols in Cell Biology. Vol. 1. J.S. Bonifacino, M. Dasso, J.B. Harford, J. Lippincot-Schawartz, and K.M. Yamada, editors. John Wiley & Sons Inc., New York. 11.0.1–11.0.2.

De La Monte, S.M., T. Luong, T.R. Neely, D. Robinson, and J.R. Wands. 2000. Mitochondrial DNA damage as a mechanism of cell loss in Alzheimer's disease. *Lab. Invest.* 80:1323–1335.

Duan, W., V.M. Rangnekar, and M.P. Mattson. 1999. Prostate apoptosis response-4 production in synaptic compartments following apoptotic and excitotoxic insults: evidence for a pivotal role in mitochondrial dysfunction and neuronal degeneration. *J. Neurochem.* 72:2312–2322.

Dunn, K.J., J.R. Perez-Polo, and T.G. Wood. 1996. Rapid neurite formation in a human cortical neuronal cell line. *Int. J. Dev. Neurosci.* 14:61–68.

Eilers, M., and G. Schatz. 1986. Binding of a specific ligand inhibits import of a purified precursor protein into mitochondria. *Nature.* 322:228–232.

Grant, S.M., S.L. Shankar, R.M. Chalmers-Redman, W.G. Tatton, M. Szyf, and A.C. Cuello. 1999. Mitochondrial abnormalities in neuroectodermal cells stably expressing human amyloid precursor protein (hAPP751). *Neuroreport.* 10:41–46.

Greenfield, J.P., J. Tsai, G.K. Gouras, B. Hai, G. Thinakaran, F. Checler, S.S. Sisodia, P. Greengard, and H. Xu. 1999. Endoplasmic reticulum and trans-Golgi network generate distinct populations of Alzheimer β-amyloid peptides. *Proc. Natl. Acad. Sci. USA.* 96:742–747.

Hasimoto, Y., T. Niikura, Y. Ito, and I. Nishimoto. 2000. Multiple mechanisms underlie neurotoxicity by different types of Alzheimer's disease mutations of amyloid precursor protein. *J. Biol. Chem.* 275:34541–34551.

Hatanpaa, K., K. Chandrasekaran, D.R. Brady, and S.I. Rapoport. 1998. No association between Alzheimer plaques and decreased levels of cytochrome oxidase subunit mRNA, a marker of neuronal energy metabolism. *Brain Res. Mol. Brain. Res.* 59:13–21.

Hugon, J., F. Esclaire, M. Lesort, G. Kisby, and P. Spencer. 1999. Toxic neuronal apoptosis and modifications of Tau and APP gene and protein expressions. *Drug Metab. Rev.* 31:635–647.

Jacobsen, J.S., A.J. Blume, and M.P. Vitek. 1991. Quantitative measurement of alternatively spliced amyloid precursor protein mRNA expression in Alzheimer's disease and normal brain by S1 nuclease protection analysis. *Neurobiol. Aging.* 12:585–592.

Janus, C., and D. Westaway. 2001. Transgenic mouse models of Alzheimer's disease. *Physiol. Behav.* 73:873–886.

Maltese, W.A., S. Wilson, Y. Tan, S. Suomensaari, S. Sinha, R. Barbour, and L. McConlogue. 2001. Retention of the Alzheimer's amyloid precursor fragment C99 in the endoplasmic reticulum prevents formation of amyloid β-peptide. *J. Biol. Chem.* 276:20267–20279.

Maurer, I., S. Zierz, and H.J. Moller. 2000. A selective defect of cytochrome c oxidase is present in brain of Alzheimer's disease patients. *Neurobiol. Aging.* 21:455–462.

Mecocci, P., A. Cherubini, M.F. Beal, R. Cecchetti, F. Chionne, M.C. Polidori, G. Romano, and U. Senin. 1996. Altered mitochondrial membrane fluidity in AD brain. *Neurosci. Lett.* 207:129–132.

Nishimura, I., T. Uetsuki, S.U. Dani, Y. Ohsawa, I. Saito, H. Okamura, Y. Uchiyama, and K. Yoshikawa. 1998. Degeneration in vivo of rat hippocampal neurons by wild-type Alzheimer amyloid precursor protein overexpressed by adenovirus-mediated gene transfer. *J. Neurosci.* 18:2387–2398.

Nunan, J., and D.H. Small. 2000. Regulation of APP cleavage by α-, β-, and γ-secretases. *FEBS Lett.* 483:6–10.

Palmert, M.R., T.E. Golde, M.L. Cohen, D.M. Kovacs, R.E. Tanzi, J.F. Gusella, M.F. Usiak, L.H. Younkin, and S.G. Younkin. 1988. Amyloid protein precursor messenger RNAs: differential expression in Alzheimer's disease. *Science.* 241:1080–1084.

Parker, W.D., Jr. 1991. Cytochrome oxidase deficiency in Alzheimer's disease. *Ann. NY Acad. Sci.* 640:59–64.

Price, D.L., and S.S. Sisodia. 1998. Mutant genes in familial Alzheimer's disease and transgenic models. *Annu. Rev. Neurosci.* 21:479–505.

Ringheim, G.E., A.M. Szcepanik, K.L. Burgher, W. Petko, J.A. Heroux, and F. Cavalieri. 1996. Transcriptional inhibition of the β-amyloid precursor protein by interferon-γ. *Biochem. Biophys. Res. Commun.* 224:246–251.

Rockenstein, E.M., L. McConlogue, H. Tan, M. Power, E. Masliah, and L. Mucke. 1995. Levels and alternative splicing of amyloid β protein precursor (APP) transcripts in brains of APP transgenic mice and humans with Alzheimer's disease. *J. Biol. Chem.* 270:28257–28267.

Robin, M.A., H.K. Anandatheerthavarada, G. Biswas, N.B. Sepuri, D.M. Gordon, D. Pain, and N.G. Avadhani. 2002. Bimodal targeting of microsomal CYP2E1 to mitochondria through activation of an N-terminal chimeric signal by cAMP-mediated phosphorylation. *J. Biol. Chem.* 277:40583–40593.

Ronnett, G.V., L.D. Hester, J.F. Nye, K. Conners, and S.H. Snyder. 1990. Human cortical neuronal cell line: establishment from a patient with unilateral megalencephaly. *Science.* 248:603–605.

Selkoe, D.J. 1999. Translating cell biology into therapeutic advances in Alzheimer's disease. *Nature.* 399:A23–A31.

Shepherd, C.E., S. Bowes, D. Parkinson, M. Cambray-Deakin, and R.C. Pearson. 2000. Expression of amyloid precursor protein in human astrocytes in vitro: isoform-specific increases following heat shock. *Neuroscience.* 99:317–325.

Sims, N.R. 1996. Energy metabolism, oxidative stress and neuronal degeneration in Alzheimer's disease. *Neurodegeneration.* 5:435–440.

Sisodia, S.S., and P.H. St George-Hyslop. 2002. γ-Secretase, Notch, Aβ and Alzheimer's disease: where do the presenilins fit in? *Nat. Rev. Neurosci.* 3:281–290.

Stephenson, D.T., K. Rash, and J.A. Clemens. 1992. Amyloid precursor protein accumulates in regions of neurodegeneration following focal cerebral ischemia in the rat. *Brain Res.* 593:128–135.

Takahashi, M., S. Dore, C.D. Ferris, T. Tomita, A. Sawa, H. Wolosker, D.R. Borchelt, T. Iwatsubo, S.H. Kim, G. Thinakaran, et al. 2000. Amyloid precursor proteins inhibit heme oxygenase activity and augment neurotoxicity in Alzheimer's disease. *Neuron.* 28:461–473.

Teller, J.K., C. Russo, L.M. DeBusk, G. Angelini, D. Zaccheo, F. Dagna-Bricarelli, P. Scartezzini, S. Bertolini, D.M. Mann, M. Tabaton, and P. Gambetti. 1996. Presence of soluble amyloid β-peptide precedes amyloid plaque formation in Down's syndrome. *Nat. Med.* 2:93–95.

Truscott, K.N., N. Pfanner, and W. Voos. 2001. Transport of proteins into mitochondria. *Rev. Physiol. Biochem. Pharmacol.* 143:81–136.

Uetsuki, T., K. Takemoto, I. Nishimura, M. Okamoto, M. Niinobe, T. Momoi, M. Miura, and K. Yoshikawa. 1999. Activation of neuronal caspase-3 by intracellular accumulation of wild-type Alzheimer amyloid precursor protein. *J. Neurosci.* 19:6955–6964.

Valla, J., J.D. Berndt, and F. Gonzalez-Lima. 2001. Energy hypo metabolism in posterior cingulate cortex of Alzheimer's patients: superficial laminar cytochrome oxidase associated with disease duration. *J. Neurosci.* 21:4923–4930.

Vijayasarathy, C., S. Damle, N. Lenka, and N.G. Avadhani. 1999. Tissue variant effects of heme inhibitors on the mouse cytochrome c oxidase gene expression and catalytic activity of the enzyme complex. *Eur. J. Biochem.* 266: 191–200.

Webster, M.T., B.R. Pearce, D.M. Bowen, and P.T. Francis. 1998. The effects of perturbed energy metabolism on the processing of amyloid precursor protein in PC12 cells. *J. Neural Transm.* 105:839–853.

Yamaguchi, H., T. Yamazaki, K. Ishiguro, M. Shoji, Y. Nakazato, and S. Hirai. 1992. Ultrastructural localization of Alzheimer amyloid b/A4 protein precursor in the cytoplasm of neurons and senile plaque-associated astrocytes. *Acta. Neuropathol. (Berl)*. 85:15–22.